Journal of Crystal Growth 425 (2015) 237–240

Contents lists available at ScienceDirect

Journal of Crystal Growth

journal homepage: www.elsevier.com/locate/jcrysgro

MBE grown GaAsBi/GaAs multiple quantum well structures: Structural and optical characterization

Robert D Richards [a,*], Faebian Bastiman [a], John S Roberts [a], Richard Beanland [b], David Walker [b], John P R David [a]

[a] Department of Electronic and Electrical Engineering, University of Sheffield, Sheffield S1 3JD, UK
[b] Department of Physics, University of Warwick, Coventry CV4 7AL, UK

ARTICLE INFO

Communicated by A. Brown
Available online 23 February 2015

Keywords:
A1. Characterization
A1. High resolution X-ray diffraction
A3. Molecular beam epitaxy
A3. Quantum wells
B1. Bismuth compounds
B2. Semiconducting gallium compounds.

ABSTRACT

A series of GaAsBi/GaAs multiple quantum well p–i–n diodes were grown by molecular beam epitaxy. Nomarski images showed evidence of sub-surface damage in each diode, with an increase in the cross-hatching associated with strain relaxation for the diodes containing more than 40 quantum wells. X-ray diffraction ω–2θ scans of the (004) reflections showed that multiple quantum well regions with clearly defined well periodicities were grown. The superlattice peaks of the diodes containing more than 40 wells were much broader than those of the other diodes. The photoluminescence spectra showed a redshift of 56 meV and an attenuation of nearly two orders of magnitude for the 54 and 63 well diodes. Calculations of the quantum confinement and strain induced band gap modifications suggest that the wells in all diodes are thinner than their intended widths and that both loss of quantum confinement and strain probably contributed to the observed redshift and attenuation in the 54 and 63 well diodes. Comparison of this data with that gathered for InGaAs/GaAs multiple quantum wells, suggests that the onset of relaxation occurs at a similar average strain–thickness product for both systems. Given the rapid band gap reduction of GaAsBi with Bi incorporation, this data suggests that GaAsBi is a promising photovoltaic material candidate.

1. Introduction

The large, non-linear bowing coefficient of Bi in GaAs [1] makes it a promising candidate for infrared detectors and the band gap temperature dependence and split-off band modification suggest applications in telecommunications [2,3]. Little attention has been paid to the potential of GaAsBi and related materials for photovoltaic (PV) applications. The large band gap reduction per unit strain on GaAs (750 meV/%strain [4,5]) makes GaAsBi/GaAs multiple quantum wells (MQWs) a candidate material system for the middle junction in triple junction PV. For this application, well numbers in excess of 60 are required [6]. GaAsBi/GaAs structures with up to 24 wells have previously been investigated [7] and this project aims to characterize structures containing up to 60 wells with a view to the development of GaAsBi as a 1 eV absorbing photovoltaic material candidate.

2. Experimental

In this work, GaAsBi/GaAs MQW p–i–n diodes were grown on 2 in. epi-ready n+ GaAs:Si substrates cleaved into 11.4 mm × 11.8 mm sections to fit the sample holder of an Omicron molecular beam epitaxy–scanning tunnelling microscopy (MBE–STM) system. Details of the sample preparation and growth calibration protocols are discussed elsewhere [8]. A 200 nm n-type GaAs:Si buffer was grown at 580 °C on each sample before the heterostructure was deposited (see Fig. 1 for sample structures). The Ga flux was 3.44 atoms $nm^{-2}\,s^{-1}$, which is equivalent to a GaAs growth rate of 0.55 μm/h, with an As_2 flux of 6 atoms $nm^{-2}\,s^{-1}$. The n-type AlGaAs cladding was also grown at 580 °C using the same Ga flux, an Al flux of 1.47 atoms $nm^{-2}\,s^{-1}$ and an As_2 flux of 7 atoms $nm^{-2}\,s^{-1}$ to produce $Al_{0.3}Ga_{0.7}As$. The sample was cooled to 380 °C and the arsenic cracker was cooled from 1000 °C to 650 °C to provide As_4 for growth of the MQW region. As_4 was used for the growth of GaAsBi because it has been shown that there is a much larger As:Ga flux ratio growth window for GaAsBi using As_4 than As_2 with no reduction in material quality [8,9]. The MQW i-region was grown using an As_4 flux of 6 atoms $nm^{-2}\,s^{-1}$. Prior to growth of the first GaAsBi well a Bi pre-layer was deposited on the growth surface. The pre-layer was deposited in the absence of a Ga flux by exposing

* Corresponding author.
E-mail address: r.richards@sheffield.ac.uk (R. Richards).

http://dx.doi.org/10.1016/j.jcrysgro.2015.02.053

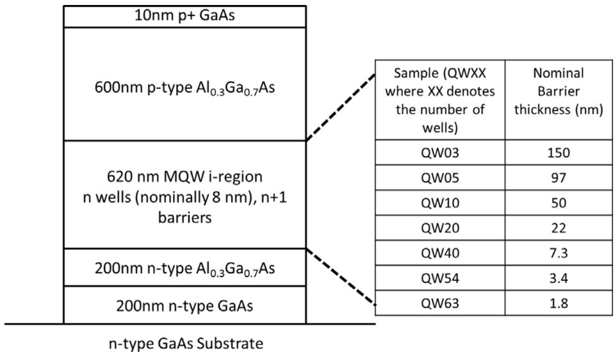

Fig. 1. Diagram of the p–i–n diode structure grown in this work. The number in each sample's name is the number of wells in that sample.

the growth surface to the same Bi flux as that used during well growth (0.24 atoms $nm^{-2}\,s^{-1}$) for 30 s. The pre-layer was intended to prevent compositional fluctuations caused by the finite time taken to build up a surface Bi layer as reported by Fan et al. [10]. After deposition of the Bi pre-layer, growth was halted for 30 s before growth of the first quantum well (QW). The nominal well thickness in every sample was 8 nm. Growth was interrupted at each well/barrier interface for 1 min to allow excess Bi (i.e. the Bi layer that forms on top of the reconstructed surface) to desorb; the Bi surface reconstruction lifetime at this temperature is significantly longer [8,10], so Bi desorption from the reconstructed Bi layer was considered to be negligible. After the growth of the QWs, the sample was heated back up to 580 °C and the As cracker was heated back up to 1000 °C to produce As_2 before deposition of the upper AlGaAs cladding and GaAs cap layers, which were grown using the same temperatures and fluxes as the first AlGaAs and GaAs layers.

The photoluminescence (PL) measurements made during this work were performed with a 532 nm continuous wave, diode pumped solid state laser. The PL signal was spectrally separated using a monochromator and the signal was passed through a phase sensitive lock-in amplifier to eliminate background noise from the measurements.

The ω–2θ X-ray diffraction (XRD) measurements throughout this work were taken on a Bruker D8 Discover XRD machine using Cu kα_1 radiation and the measured diffraction patterns were modelled using RADS Mercury software assuming a GaBi lattice constant of 6.28 Å [11].

3. Results

3.1. Nomarski

Nomarski differential interference microscopy images of the surfaces of the diodes (Fig. 2) showed signs of sub-surface structural damage. For the diodes with up to 40 wells, the sub-surface damage lines were not all orthogonal and straight, so it seems unlikely that they were caused by strain relaxation [12]. QW54 and QW63 showed a much greater density of damage lines and a significant proportion of the lines were straight and orthogonal, indicating that strain relaxation may have played a part in their formation.

3.2. XRD

Initial (004) XRD scans of the diodes are shown in Fig. 3. The presence of clear superlattice (SL) peaks indicates that MQW regions of well-defined periodicity were formed. There is a significant broadening of the SL peaks for QW54 and QW63, which is often an indication of strain relaxation [14]. As only the symmetrical 004 scan was performed on these diodes, only the MQW period and average Bi content have been extracted from this data, assuming no strain relaxation. By assuming 8 nm wells of uniform Bi content, the measured MQW period and average Bi content were used to calculate the average strain in the MQW region. The predicted average strain was calculated using the nominal well and barrier thicknesses. The predicted average strain most accurately matched the measured average strain when the Bi content was set to be 2.83%.

3.3. PL

The PL spectra from the diodes grown in this work are shown in Fig. 4. The diodes with up to 40 wells show a slight variation in peak position and peak intensity. This variation is probably due to variations in the substrate temperature and atomic fluxes during growth. The growth temperature uncertainty is ± 10 °C, the flux uncertainties are all $\pm$ 10%, and Bi incorporation is very sensitive to the growth temperature and atomic fluxes during growth [8].

The diodes containing more than 40 wells show a significant redshift and attenuation of their PL spectra. The redshift between the mean PL peak energies of the diodes with up to 40 wells and those with more than 40 wells is 56 meV. The significant redshift and attenuation of the spectra from QW54 and QW63 could be caused by two effects: strain relaxation and loss of quantum confinement. The redshift associated with each effect was calculated to determine which was responsible for the observed redshift and attenuation in the PL spectra.

3.4. Analysis

From the Nomarski, XRD and PL data, there appears to have been a strain relaxation event in QW54 and QW63. The analysis was, therefore, only conducted for the diodes with up to 40 wells as the average strain estimated from the XRD data and the Bi content estimated from the PL spectra would be affected by relaxation.

First, the quantum confinement energy in each sample was calculated assuming a uniform Bi content throughout the QWs. This assumption was necessary to complete the calculations; however, it has been shown that GaAsBi QWs do not always have uniform Bi contents [15]. The numbers derived from these calculations are, therefore, only effective well widths and Bi contents, which are used to estimate the quantum confinement and band gap modification due to strain in each diode. By varying the estimated QW widths and Bi contents in each diode in order to match the first calculated QW transition to the observed peak PL energy (as in Fig. 4), while maintaining the observed average strain in the MQW region (as in Fig. 3b), new estimates of the average QW width, Bi content and quantum confinement energy in each MQW were obtained. These parameters were then used to estimate the redshift of the first QW transition associated with a total loss of strain in the MQW region. The calculations were performed using the finite QW confinement energy estimates of Singh [16], electron and hole reduced masses of $0.06m_0$ [17] and $0.55m_0$ [18] respectively and the calculations of the effect of strain on the band structure of GaAsBi by Batool et al. [19]. The results are shown in Table 1. All of the calculated well widths are thinner than expected. TEM images like that shown in Fig. 5 suggest that the well thicknesses are around 4.8 ± 0.6 nm. It is probable that the wells are not uniform in profile, which would explain why the calculated well thicknesses are larger than the thickness estimated from TEM.

It seems likely that a relaxation event has occurred in QW54 and QW63 from the XRD and Nomarski measurements and the calculated redshift associated with the complete relaxation of strain in the other MQWs is sufficient to account for the observed redshift in the PL spectra of these samples (56 meV) as seen in Table 1. However, the estimated quantum confinement energy in each MQW is also sufficient to account for the observed redshift. These

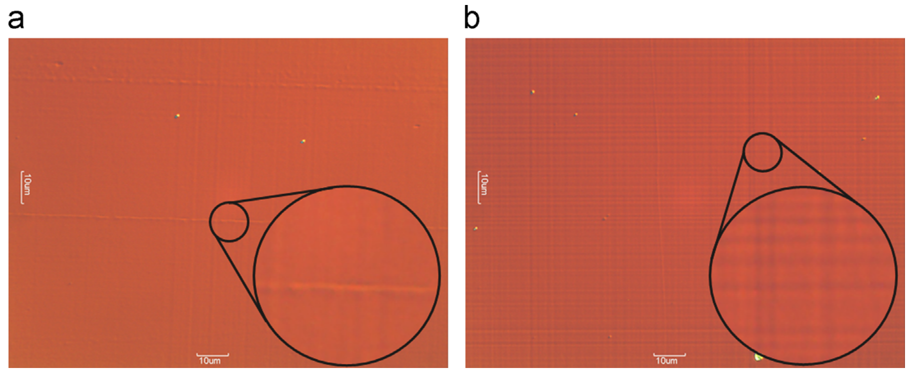

Fig. 2. Nomarski images of a) QW40 and b) QW54.

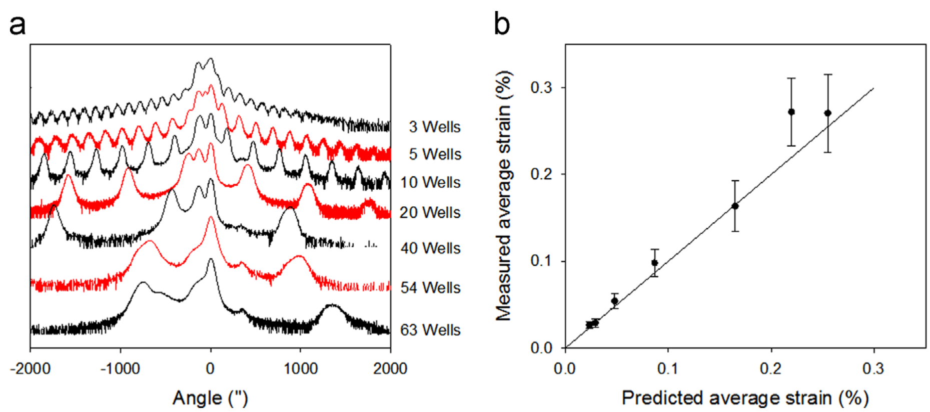

Fig. 3. Data from the initial XRD characterization of the diodes. a) (004) ω–2θ scans of each diode, the y-axis is on a log scale and the scans have been vertically offset for clarity and b) the average strain in each MQW region measured by XRD, plotted against the estimated average strain in each MQW region assuming 8 nm wells of 2.83% Bi. The calculations were performed using the method of Ref. [13]. The error bars were estimated from the range of Bi contents that produced a reasonable fit between the measured and modelled XRD scans.

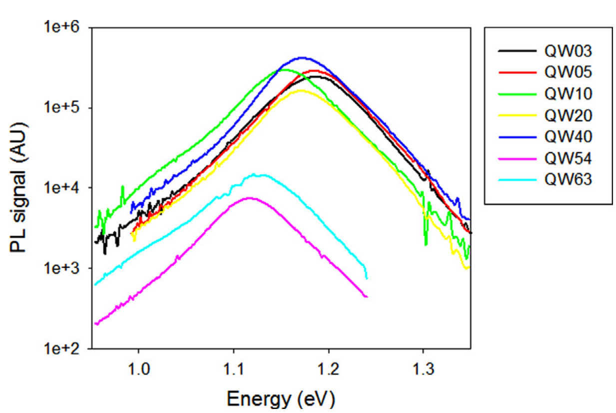

Fig. 4. PL spectra from all diodes in this work.

estimates represent upper limits of the redshift associated with each effect. In practice, it is unlikely that either quantum confinement or strain will be completely lost. Therefore, it seems reasonable to assume that both effects contribute to the redshift of the PL spectra from QW54 and QW63. Further investigation is required to differentiate between the two effects in these layers.

The greatest number of wells grown before the onset of strain relaxation in this work was 40, at a band gap of around 1.18 eV. The mean well width in this work is 5.6 nm and, in order to reach 1 eV, the Bi content of 5.6 nm wells would need to be ~8%. The maximum number of such wells that could be contained in a 620 nm MQW without dislocation multiplication is around 30. Strain balancing will be required to realise thicker GaAsBi/GaAs MQWs.

Table 1
Well widths, Bi contents, quantum confinement energies, and strain induced band gap modifications for each diode in this work. QW54 and QW63 were omitted as the MQW regions in these diodes are expected to have relaxed. The uncertainties associated with the parameters in this table are derived from the uncertainties in the average strain in each MQW as shown in Fig. 3 and the uncertainty in the estimate of the band gap from the PL spectra.

Sample	Estimated well width (nm)	Estimated Bi content (%)	Estimated quantum confinement energy (meV)	Estimated band gap modification due to strain (meV)	Estimated first transition blueshift due to strain (meV)
QW03	6.4 ± 1.0	4.0 ± 0.5	59 ± 11	62 ± 8	51 ± 16
QW05	5.3 ± 0.9	4.8 ± 0.5	75 ± 13	66 ± 9	50 ± 17
QW10	5.3 ± 1.0	4.2 ± 0.5	67 ± 13	76 ± 11	61 ± 20
QW20	5.8 ± 0.9	4.4 ± 0.5	66 ± 12	69 ± 9	53 ± 17
QW40	5.0 ± 0.9	4.5 ± 0.5	73 ± 14	71 ± 9	57 ± 19

3.5. Comparison with InGaAs/GaAs

The results from this work are compared to those of Griffin et al. [13] from the InGaAs/GaAs material system in Fig. 6. It seems that GaAsBi/GaAs MQWs undergo strain relaxation at a similar average strain–thickness product to InGaAs/GaAs MQWs. The samples analysed by Griffin et al. were grown at 500 °C [21] and the low growth temperature used for the GaAsBi layers in this work could freeze defects into the MQW regions and make them seem less susceptible to strain relaxation. Even so, this data suggests that GaAsBi could be a suitable alternative to InGaAs for PV applications

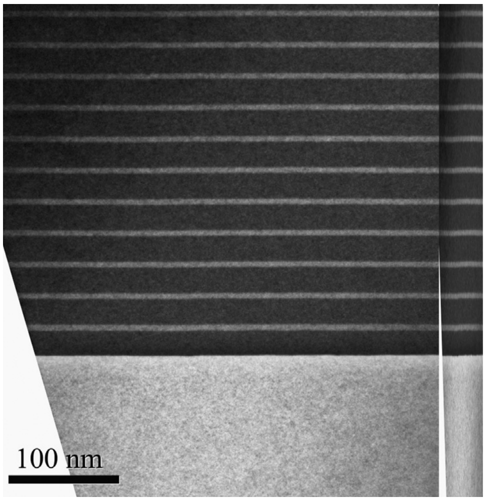

Fig. 5. Dark field TEM image of QW20.

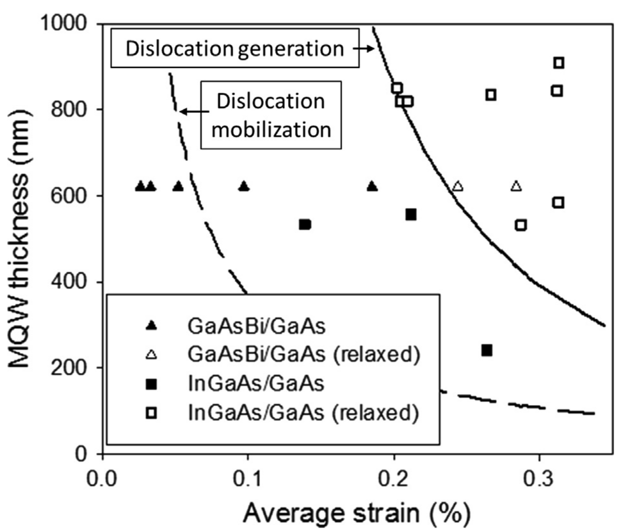

Fig. 6. Plot of the thicknesses and average strains of the samples reported by Griffin et al. [13]. The dashed line is the calculated Matthews–Blakeslee critical thickness for dislocation propagation; the solid line is the dislocation generation critical thickness taken from the data of Drigo et al. [20]; the squares represent InGaAs/GaAs MQWs; the triangles represent GaAsBi/GaAs MQWs; and the empty symbols represent samples which exhibit significant relaxation.

as the rapid reduction in band gap with Bi incorporation allows for better tailoring of the absorption edge of the material.

4. Conclusions

GaAsBi/GaAs MQW diodes were grown. Nomarski images of the sample surfaces and XRD ω–2θ measurements suggest that lattice relaxation occurred in the diodes with more than 40 wells. The PL spectra from the diodes with more than 40 wells show a redshift and attenuation compared to the other diodes. Calculations of the quantum confinement energies and strain induced band gap modifications of each diode suggest that strain relaxation and a loss of quantum confinement have occurred in the diodes with more than 40 QWs. The GaAsBi/GaAs MQWs appear to relax at a similar average strain–thickness product to InGaAs/GaAs MQWs. This suggests that replacing InGaAs with GaAsBi in multi-junction photovoltaics could produce a middle junction with a better optimized band gap. However, strain balancing with a material such as GaAsP needs to be investigated. Further work is also required to assess the electrical characteristics of these diodes for their suitability for photovoltaic applications.

Acknowledgements

The work of R.D. Richards was supported in part by the E-Futures Doctoral Training Centre which is funded by the RCUK Energy Programme (reference number: EP/G037477/1; http://gow.epsrc.ac.uk/NGBOViewGrant.aspx?GrantRef=EP/G037477/1).

References

[1] T. Tiedje, E.C. Young, A. Mascarenhas, Growth and properties of the dilute bismide semiconductor GaAs1–*x*Bi*x* a complementary alloy to the dilute nitrides, Int. J. Nanotechnol. 5 (9–12) (2008) 963–983.
[2] S.J. Sweeney, S.R. Jin, Bismide-nitride alloys: promising for efficient light emitting devices in the near- and mid-infrared, J. Appl. Phys. 113 (4) (2013) 043110.
[3] C.A. Broderick, et al., Band engineering in dilute nitride and bismide semiconductor lasers, Semicond. Sci. Technol. 27 (2012) 9.
[4] S. Francoeur, et al., Band gap of $GaAs_{1-x}Bi_x$, $0<x<3.6\%$, Appl. Phys. Lett. 82 (22) (2003) 3874–3876.
[5] S. Tixier, et al., Molecular beam epitaxy growth of $GaAs_{1-x}Bi_x$, Appl. Phys. Lett. 82 (14) (2003) 2245–2247.
[6] D.B. Bushnell, et al., Effect of well number on the performance of quantum-well solar cells, J. Appl. Phys. 97 (12) (2005) 124908–124911.
[7] Y. Tominaga, et al., Structural investigation of $GaAs_{1-x}Bi_x$/GaAs multiquantum wells, Appl. Phys. Lett. 93 (13) (2008) 131915.
[8] R.D. Richards, et al., Molecular beam epitaxy growth of GaAsBi using As_2 and As_4, J. Cryst. Growth 390 (0) (2014) 120–124.
[9] F. Bastiman, et al., Non-stoichiometric GaAsBi/GaAs (100) molecular beam epitaxy growth, J. Cryst. Growth 338 (1) (2012) 57–61.
[10] D. Fan, et al., MBE grown GaAsBi/GaAs double quantum well separate confinement heterostructures, J. Vac. Sci. Technol. B: Microelectron. Nanometer Struct. 31 (3) (2013) 181103–181106.
[11] H. Achour, et al., Structural and electronic properties of GaAsBi, Superlattices Microstruct. 44 (2) (2008) 223–229.
[12] D.J. Dunstan, Strain and strain relaxation in semiconductors, J. Mater. Sci.: Mater. Electron. 8 (6) (1997) 337–375.
[13] P.R. Griffin, et al., Effect of strain relaxation on forward bias dark currents in GaAs/InGaAs multiquantum well p-i-n diodes, J. Appl. Phys. 80 (10) (1996) 5815–5820.
[14] P.F. Fewster, X-ray diffraction from low-dimensional structures, Semicond. Sci. Technol. 8 (11) (1993) 1915.
[15] Y.I. Mazur, et al., Effects of spatial confinement and layer disorder in photoluminescence of $GaAs_{1-x}Bi_x$/GaAs heterostructures, J. Phys. D: Appl. Phys. 46 (6) (2013) 065306–065313.
[16] J. Singh, Analytical closed form expressions for the effective band edges in shallow quantum wells, Appl. Phys. Lett. 64 (20) (1994) 2694–2696.
[17] B. Fluegel, et al., *Shubnikov-de Haas measurement of electron effective mass in* $GaAs_{1-x}Bi_x$, Appl. Phys. Lett. 99 (16) (2011) 162108–162108-3.
[18] J. Hwang, J.D. Phillips, Band structure of strain-balanced GaAsBi/GaAsN superlattices on GaAs, Phys. Rev. B 83 (19) (2011) 195327.
[19] Z. Batool, et al., The electronic band structure of GaBiAs/GaAs layers: influence of strain and band anti-crossing, J. Appl. Phys. 111 (11) (2012) 113108.
[20] A.V. Drigo, et al., On the mechanisms of strain release in molecular-beam-epitaxy-grown $In_xGa_{1-x}As$/GaAs single heterostructures, J. Appl. Phys. 66 (5) (1989) 1975–1983.
[21] J.P.R. David, et al., Barrier width dependence of leakage currents in InGaAs/GaAs multiple quantum-well P-I-N-diodes, J. Electron. Mater. 20 (4) (1991) 295–297.